

Grass waste: A novel sorbent for the removal of basic dye from aqueous solution

B.H. Hameed*

School of Chemical Engineering, Engineering Campus, University of Science Malaysia, 14300 Nibong Tebal, Penang, Malaysia

ARTICLE INFO

Article history:

Received 3 June 2008

Received in revised form

10 November 2008

Accepted 10 November 2008

Available online 17 November 2008

Keywords:

Grass waste

Adsorption

Isotherm

Methylene blue

Kinetics

ABSTRACT

The aim of the present work was to investigate the feasibility of grass waste (GW) for methylene blue (MB) adsorption. The adsorption of MB on GW material was studied as a function of GW dose (0.05–1.20 g), solution pH 3–10, contact time and initial concentration (70–380 mg/L). The influence of these parameters on the adsorption capacity was studied using the batch process. The experimental data were analyzed by the Langmuir and Freundlich isotherms. The adsorption isotherm was found to follow the Langmuir model. The monolayer adsorption capacity was found to be 457.640 mg/g. The kinetic data were fitted to the pseudo-first-order and pseudo-second-order models, and were found to follow closely the pseudo-second-order kinetic model. The results revealed that GW adsorbent is potentially low-cost adsorbent for adsorption of MB.

© 2008 Elsevier B.V. All rights reserved.

1. Introduction

Treatment of effluent from textile and related industries is considered a global environmental issue. Effluent derived from the textile and dyestuff activities can provoke serious environmental impact on the neighboring receptor water bodies because of the presence of toxic reactive dyes, chlorolignin residues and dark coloration [1]. There are many treatment processes applied for the removal of dyes from wastewater. A critical review on current treatment technologies with a proposed alternative was reported by Robinson et al., [2] and Ramesh Babu et al., [3].

Removal of dyes from wastewater using adsorption on commercial activated carbons is a very effective process, but the high cost of such adsorbent has motivated the search for alternatives and low-cost adsorbents. Recently, many researchers attempted to use alternative low-cost adsorbents to substitute the more expensive, commercially available activated carbons. Such alternative include: biosorbents, natural materials, and agricultural waste and industrial by-products. Table 1 listed some of the reported adsorbents used for removal of dyes from aqueous solutions. An extensive list of sorbent literature for dye removal has been compiled recently by Crini [18].

In this work, an attempt to use grass waste, as a novel non-conventional low-cost adsorbent for removal of methylene blue (MB) from aqueous solution has been made. Grass and yard waste are a major organic component of the solid waste, comprising about

14.6% of total municipal solid waste (MSW) and about 50% of the organic fraction of the MSW [19]. Malaysia, with no winter, plenty of sunshine, rainfall and a constantly humid environment, has the world's highest rate of biomass production; and therefore, generates huge quantities of organic wastes, such as grass, leaves and flowers. To make better use of this abundant agricultural waste, this present study was carried out to propose its use as adsorbent for removal of basic dye from aqueous solutions. Thus, the purpose of the present work was to evaluate the adsorption potential of grass waste for the removal of methylene blue from aqueous solution.

2. Materials and methods

2.1. Methylene blue and stock solution

Methylene blue (MB) purchased from Sigma–Aldrich (M) Sdn Bhd, Malaysia was used as model adsorbate. A stock solution of 1000 mg/L was prepared by dissolving an appropriate quantity of MB in a liter of distilled water. The working solutions were prepared by diluting the stock solution with distilled water to give the appropriate concentration of the working solutions.

2.2. Analytical methods

Prior to the measurement, a calibration curve was obtained by using the standard MB solution with the known concentrations. The concentration of the residual dye was measured using a double beam UV–vis spectrophotometer (Shimadzu, Model UV 1601, Japan) at a λ_{\max} corresponding to the maximum absorption for the dye solution ($\lambda_{\max} = 668 \text{ nm}$) by withdrawing samples at fixed time

* Tel.: +60 4 599 6422.

E-mail address: chbassim@eng.usm.my.

Table 1
Recent research on adsorption of dyes by different adsorbents.

Adsorbent	Dye investigated	Max. adsorption capacities (mg/g)	Reference
Grass waste	Methylene blue	457.640	This work
<i>Luffa cylindrica</i> fibers	Methylene blue	47	[4]
<i>Caulerpa racemosa</i> var. <i>cylindracea</i>	Methylene blue	3.423	[5]
Solis waste of soda ash plant	Reactive red 231	667	[6]
Chitosan bead	Malachite green	93.55	[7]
Biomass fly ash (FA-BM)	Reactive black 5	4.38	[8]
Biomass fly ash (FA-BM)	Reactive yellow 176	3.65	[8]
Castor seed shell	Methylene blue	158.73	[9]
Chitosan-based adsorbent	Basic blue 3	166.5	[10]
Untreated desert plant	Methylene blue	23	[11]
Pyrolyzed desert plant	Methylene blue	53	[11]
Chemically activated desert plant	Methylene blue	130	[11]
Untreated guava leaves	Methylene blue	295	[12]
Yellow passion fruit waste	Methylene blue	44.70	[13]
Oil palm trunk fibre	Malachite green	149.35	[14]
Sunflower seed hull	Methyl violet	92.59	[15]
Broad bean peels	Methylene blue	192.7	[16]
Soy meal hull	Direct red 80	178.57	[17]
Soy meal hull	Direct red 81	120.482	[17]
Soy meal hull	Acid blue 92	114.943	[17]
Soy meal hull	Acid red 14	109.89	[17]

intervals, filtered using 0.45 μm filter paper (Whatman, UK), and the supernatant was analyzed for residual MB.

2.3. Preparation and characterization of grass waste adsorbent

The grass waste (GW) was collected from the field of the Engineering Campus, University of Science Malaysia, Malaysia. It was washed, dried, crushed and sieved to desired mesh size (250–355 μm). The sample was stored in an airtight container for further use. No other chemical or physical treatments were used prior to adsorption experiments. Scanning electron microscopy (SEM) analysis was carried out for the GW before and after MB adsorption to study the surface morphology. The analysis was carried out using a scanning electron microscope (Leo Supra, Model 50VP Field Emission, UK). The sample was put on the carbon tape on the aluminum stub and coated with gold for electron reflection. The sample was then vacuumed for 5–10 min before analysis. The functional groups available on the surface of the GW before and after MB adsorption were detected by KBr technique using a Fourier Transform Infrared (FTIR) spectroscope (PerkinElmer, Model FTIR-2000, US). The spectra were recorded from 4000 to 400 cm^{-1} .

2.4. Equilibrium and kinetic studies

Adsorption equilibrium and kinetics studies were determined by batch method. Adsorption equilibrium experiments were carried out by adding a fixed amount of adsorbent (0.70 g) into a number of 250 mL-stoppered glass (Erlenmeyers flasks) containing a definite volume (200 mL in each case) of different initial concentrations (70–380 mg/L) of dye solution without changing pH and temperature 30 °C. The flasks were placed in a thermostated water-bath shaker and agitation was provided at 130 rpm for 180 min.

The amount of adsorption at equilibrium, q_e (mg/g), was calculated by:

$$q_e = \frac{(C_0 - C_e)V}{W} \quad (1)$$

where C_0 and C_e (mg/L) are the liquid-phase concentrations of dye at initial and equilibrium, respectively. V (L) is the volume of the solution and W (g) is the mass of dry sorbent used.

The dye removal percentage can be calculated as follows:

$$\text{Removal percentage} = \left(\frac{C_0 - C_e}{C_0} \right) \times 100 \quad (2)$$

To study the effect of GW dose on the amount of MB adsorbed, different amounts of GW (0.05, 0.10, 0.15, 0.20, 0.40, 0.60, 0.80, 1.00 and 1.20 g) were respectively added into a number of 250 mL-stoppered glass (Erlenmeyers flasks) containing a definite volume (200 mL in each flask) of fixed initial concentration (70 mg/L) of dye solution without changing the solution pH at temperature of 30 °C. The flasks were placed in a thermostated water-bath shaker and agitation was provided at 130 rpm for 180 min. The dye concentrations were measured at equilibrium.

To study the effect of solution pH, 200 mL of dye solution of 70 mg/L initial concentration at different pH values (3.0–10.0) was agitated with 0.70 g of GW in a water-bath shaker at 30 °C. Agitation was made for 180 min at a constant agitation speed of 130 rpm. The pH was adjusted with 0.1 N NaOH and 0.1 N HCl solutions and measured by using a pH meter (Ecoscan, EUTECH Instruments, Singapore).

The procedures of kinetic experiments were basically identical to those of equilibrium tests. The aqueous samples were taken at preset time intervals, and the concentrations of dye were similarly measured. All the kinetic experiments were carried out at 30 °C. The amount of sorption at time t , q_t (mg/g), was calculated by:

$$q_t = \frac{(C_0 - C_t)V}{W} \quad (3)$$

where C_t (mg/L) is the liquid-phase concentrations of dye at any time.

3. Results and discussion

3.1. Effect of adsorbent dose on dye adsorption

To study the effect of GW dose (g) on MB adsorption, experiments were conducted at initial MB of 70 mg/L, while the amount of adsorbent added was varied. Fig. 1 shows the effect of adsorbent dose on the % removal of MB. It was observed that the % removal of MB rapidly increased with the increase in adsorbent dose up to 0.20 g, then gradually increased with further increase in adsorbent dose up to 0.60 g and thereafter remained unchanged. At equilibrium time, the % removal increased from 17.74 to 77.66% for an increase in GW dose from 0.05 to 0.60 g. The increase in % color removal was due to the increase in the available sorption surface sites.

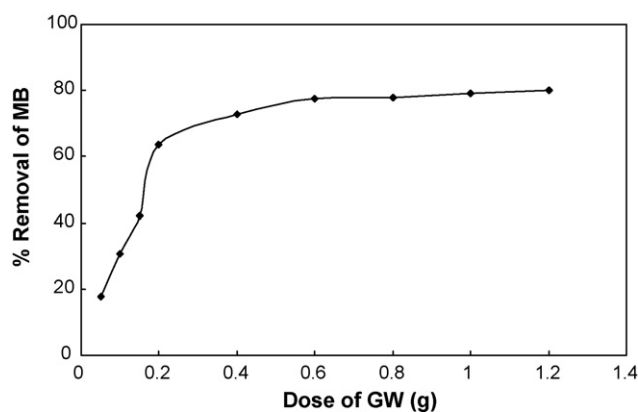


Fig. 1. Effect of adsorbent dosage on the adsorption of MB on GW.

3.2. Effect of solution pH on dye uptake

To study the effect of solution pH on equilibrium uptake capacity of GW, experiments were conducted at 70 mg/L initial MB concentration, 0.70 g GW dose and 30 °C. Fig. 2 shows that the sorption of MB was minimum at the initial pH 3 and increased with pH up to 5 and then remained constant over the initial pH ranges of 5–10. The observed low adsorption rate of MB on the GW at pH 5 may be because the surface charge became positively charged, thus making (H^+) ions compete effectively with dye cations causing a decrease in the amount of dye adsorbed. When the solution pH increased, the positive charge on the solution interface decreased and the adsorbent surface appeared to be negatively charged. A similar behavior was observed for malachite green adsorption on rice straw-derived char [20]. Several investigations carried out on adsorption of MB on various adsorbents have as well shown that the adsorption of MB preferred higher solution pH values. However, the level of influence of the solution pH on the adsorption capacity might vary, depending on the adsorbent–adsorbate system. The adsorbents which had been reported were such as wheat shells [21], coir pith carbon [22], clay [23] and commercial activated carbon F400 from Calgon, US [24].

3.3. Effect of contact time and initial concentration

The effect of MB initial concentration was studied using a range of MB concentrations between 70–380 mg/L at a fixed adsorbent dosage (0.70 g), shaker speed (130 rpm) at 30 °C. Fig. 3 shows the result for effect of initial concentration on adsorption of MB onto GW. The plots of Fig. 3 can be divided into three distinct regions: (1) rapid adsorption during the first 20 min, (2) gradual equilibrium till the equilibrium state for each concentration and (3) the equilibrium state. The result indicates that an increase in initial MB concentra-

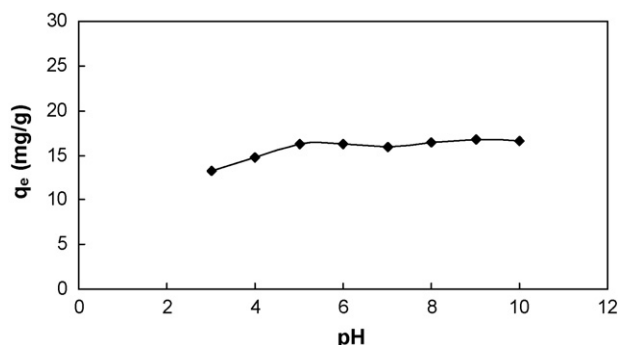


Fig. 2. Effect of pH on equilibrium uptake of MB.

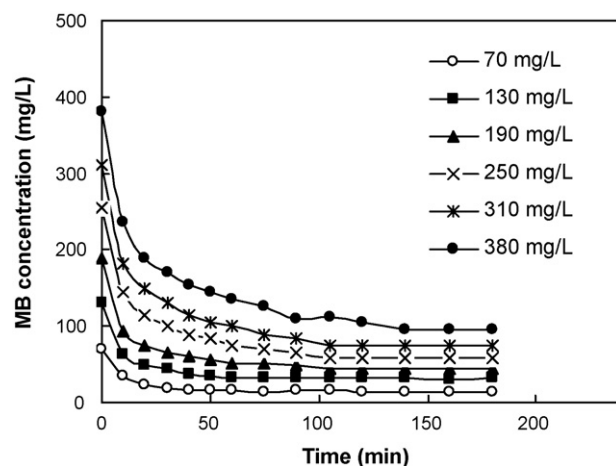


Fig. 3. Effect of initial concentration and contact time on MB adsorption.

tion leads to increase in the adsorption of MB on GW. At equilibrium, MB adsorption increased from 16.41 to 80.63 mg/g, with increase in the initial MB concentration from 70 to 380 mg/L. As the initial MB concentration increased from 70 to 380 mg/L the equilibrium removal of MB decreased from 79.23 to 74.77 %. This was because when the initial concentration increased, the mass transfer driving force would become larger, hence resulting in higher MB adsorption. Similar trend was obtained in the adsorption of MB on flyash [25] and also commercial activated carbon [26].

At initial concentration (70–130 mg/L), the system achieved adsorption equilibrium in less than 40 min. While at high initial MB concentration (190–380 mg/L), the time necessary to reach equilibrium was 140 min. However, the experimental data were measured at 180 min to be sure that full equilibrium was attained. This observation could be explained by the theory that in the process of dye adsorption, initially the dye molecules have to first encounter the boundary layer effect and then diffuse from the boundary layer film onto adsorbent surface and then finally, they have to diffuse into the porous structure of the adsorbent [27,28]. Therefore, MB solutions of higher initial concentrations will take relatively longer contact time to attain equilibrium due to higher amount of dye molecules.

3.4. Isotherm analysis

A set of batch experiments was carried out at different MB concentrations varying from 70–380 mg/L. Other process parameters were kept constant: 0.70 g GW dose, 130 rpm shaker speed, 0.20 L solution volume and 30 °C. The results of the equilibrium isotherms were analyzed using the Langmuir [29] and Freundlich [30] isotherms. A trial and error procedure was used to determine the isotherm parameters by minimizing the respective coefficient of determination between experimental data and isotherms using the solver add-in with Microsoft's Excel spreadsheet.

The Langmuir isotherm theory assumes monolayer coverage of adsorbate over a homogenous adsorbent surface [29]. A basic assumption is that sorption takes place at specific homogeneous sites within the adsorbent. Once a dye molecule occupies a site, no further adsorption can take place at that site. The Langmuir isotherm is [29]:

$$q_e = \frac{q_m K_a C_e}{1 + K_a C_e} \quad (4)$$

where q_m (mg/g) and K_a (L/mg) are the Langmuir isotherm constants. The Langmuir isotherm model has been successfully applied to many adsorption processes [31,32,16]. The equilibrium data were fitted to Langmuir isotherm and the constants together with the R^2

Table 2
Isotherm parameters for removal of MB on GW.

Isotherms	Parameters	Value
Langmuir	Q_0 (mg/g)	457.640
	K_d	0.0023
	R^2	0.9975
Freundlich	K_F	1.423
	n	1.123
	R^2	0.9970

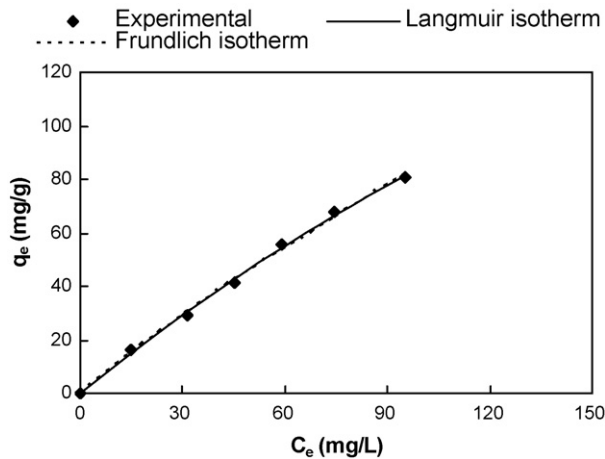


Fig. 4. Isotherm plots for MB adsorption on GW.

value are listed in Table 2. Fig. 4 shows the experimental equilibrium data and the predicted theoretical Langmuir isotherm.

The essential characteristics of the Langmuir isotherm can be expressed in terms of a dimensionless constant separation factor R_L that is given by Eq. (5) [33]:

$$R_L = \frac{1}{(1 + K_d C_0)} \quad (5)$$

where C_0 (mg/L) is the highest initial concentration of adsorbate, and K_d (L/mg) is Langmuir constant. The value of R_L indicates the shape of the isotherm to be either unfavorable ($R_L > 1$), linear ($R_L = 1$), favorable ($0 < R_L < 1$), or irreversible ($R_L = 0$). The R_L values between 0 and 1 indicate favorable adsorption. For adsorption of MB onto GW, R_L values obtained as shown in Fig. 5 are in the range of 0.534–0.861, indicating that the adsorption is a favorable process.

The Freundlich isotherm [30] is an empirical equation assuming that the adsorption process takes place on heterogeneous surfaces and adsorption capacity is related to the concentration of MB dye

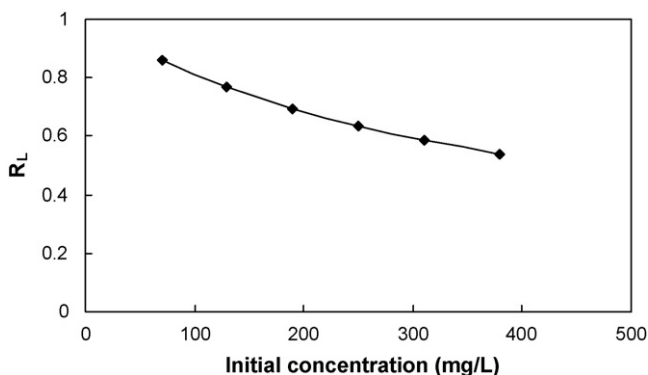


Fig. 5. The separation factor for MB adsorption on GW.

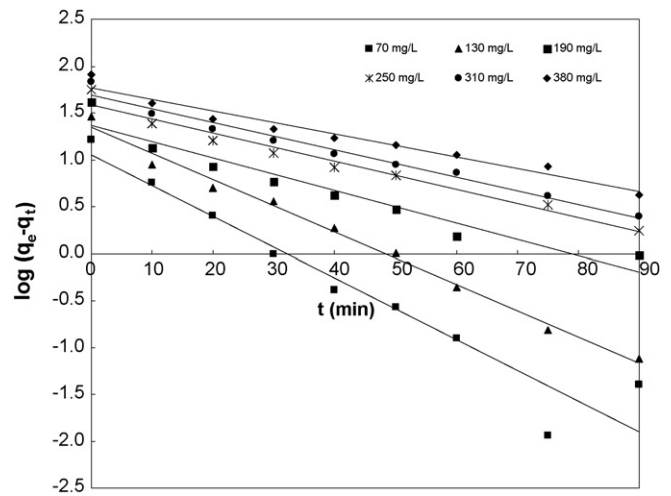


Fig. 6. Pseudo-first-order kinetic for adsorption of MB on GW.

at equilibrium:

$$q_e = K_F C_e^{1/n} \quad (6)$$

where K_F (mg/g (L/mg) $^{1/n}$) is roughly an indicator of the adsorption capacity and $1/n$ is the adsorption intensity. The magnitude of the exponent, $1/n$, gives an indication of the favorability of adsorption. Values of $n > 1$ represent favorable adsorption condition [34,35]. The values of K_F , n and R^2 for Freundlich isotherm are given in Table 2. Fig. 4 shows the experimental equilibrium data and the predicted theoretical Freundlich isotherm. The isotherm parameters and R^2 values determined by non-linear regression are presented in Table 2. Based on the R^2 values, the data fitted well with Langmuir isotherm with R^2 of 0.9975.

Table 1 presents the comparison of adsorption capacity of GW for MB ($q_m = 457.64$ mg/g) with that of several other low-cost adsorbents reported in literature. A direct comparison with different MB/adsorbents listed in Table 1 is not possible because the properties of adsorbents and experimental conditions used are different. However, it can be concluded that the adsorption capacity of GW found in this work was comparable to those adsorbents for cationic dye removal.

3.5. Adsorption kinetics

The experimental data for the adsorption of MB on GW were fitted using the pseudo-first-order (Eq. (7)) [36] and pseudo-second-order kinetic models (Eq. (8)) [37]:

$$\log(q_e - q_t) = \log q_e - \frac{k_1}{2.303} t \quad (7)$$

$$\frac{t}{q_t} = \frac{1}{k_2 q_e^2} + \frac{1}{q_e} t \quad (8)$$

where q_e (mg/g) is the amount of adsorbate adsorbed at equilibrium, q_t (mg/g) is the amount of adsorbate adsorbed at time t , k_1 (1/min) is the rate constant of pseudo-first-order adsorption, k_2 (g/mg.min) is the rate constant of pseudo-second-order adsorption.

The straight-line plots of $\log(q_e - q_t)$ versus t (Fig. 6) for the adsorption of MB onto GW have also been tested to obtain the rate parameters. The k_1 , $q_{e,cal}$ and correlation coefficients R^2 under different MB concentrations were calculated from these plots and are listed in Table 3. The correlation coefficients R^2 listed in Table 3 for the first-order kinetic model were ≥ 0.9206 .

Fig. 7 shows plots between (t/q_t) versus t . The k_2 and $q_{e,cal}$ values, computed from Eq. (8) along with correlation coefficients R^2 are listed in Table 3. The R^2 values obtained for this model were above

Table 3Comparison of the pseudo-first-order and pseudo-second-order adsorption rate constants, and calculated and experimental q_e values for different initial MB concentrations.

C_0 (mg/L)	Pseudo-first-order kinetic model				Pseudo-second-order kinetic model			
	k_1 (1/min)	$q_{e,cal.}$ (mg/g)	R^2	Δq (%)	k_2 (g/mg min)	$q_{e,cal.}$ (mg/g)	R^2	Δq (%)
70	0.0755	11.3058	0.9206	34.49	0.0120	17.4520	0.9988	3.67
130	0.0336	49.0682	0.9783	55.70	0.0057	30.7692	0.9996	1.89
190	0.0348	38.4592	0.9717	25.36	0.0038	43.2900	0.9997	1.26
250	0.0398	23.1366	0.9300	63.83	0.0017	59.5238	0.9994	1.91
310	0.0643	22.1360	0.9913	69.05	0.0012	72.9927	0.9990	2.42
380	0.0283	58.1969	0.9608	38.89	0.0009	84.7458	0.9973	2.84

0.9973 for all concentrations studied, which were higher than the R^2 values obtained for the pseudo-first-order model.

In order to quantitatively compare the applicability of the model in fitting the data, a normalized standard deviation, Δq , was calculated from Eq. (9).

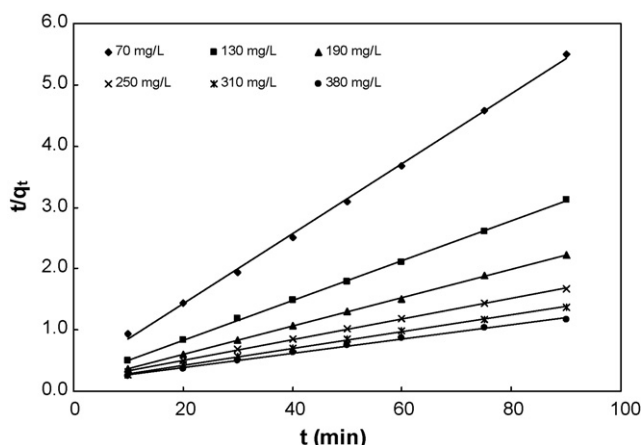
$$\Delta q(\%) = 100 \times \sqrt{\frac{\sum [(q_{t,exp} - q_{t,cal})/q_{t,exp}]^2}{(n-1)}} \quad (9)$$

where the $q_{t,exp}$ and $q_{t,cal}$ refer to the experimental and calculated values and n is the number of data points. The calculated $q_{e,cal}$ values obtained from the pseudo-first-order kinetic model did not give reasonable values, showing relatively large Δq values of 25.36–69.05%. Thus the experimental results did not follow the first-order kinetic model. However, for pseudo-second-order kinetic, the calculated $q_{e,cal}$ values agreed with experimental $q_{e,exp}$ values, giving relatively small deviation of 1.26–3.67%, besides the linear regression coefficients were close to 1.00. Therefore, it can be concluded that the kinetics of MB adsorption on GW followed pseudo-second-order model, suggesting that chemisorption might be the rate-limiting step that controlled the adsorption process.

3.6. Intraparticle diffusion study

In order to investigate the mechanism of the MB adsorption onto GW, intraparticle diffusion based mechanism was studied. The most commonly used technique for identifying the mechanism involved in the adsorption process is by fitting an intraparticle diffusion plot. It is an empirically found functional relationship, common to most adsorption processes, where uptake varies almost proportionally with $t^{1/2}$ rather than with the contact time t . According to the theory proposed by Weber and Morris [38]:

$$q_t = k_{pi}t^{1/2} + C_i \quad (10)$$

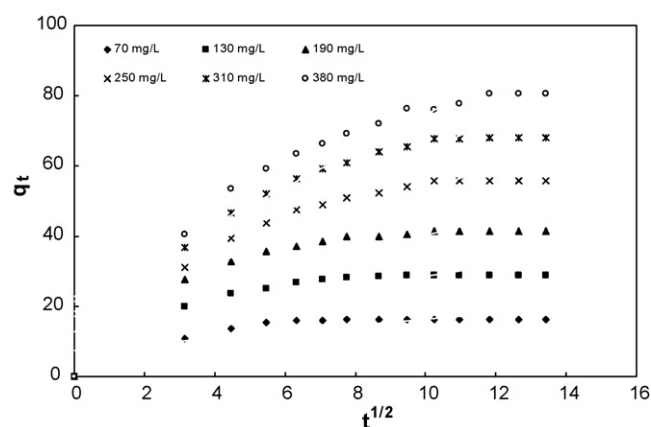
**Fig. 7.** Pseudo-second-order kinetic for adsorption of MB on GW.

where k_{pi} (mg/g min^{1/2}), the rate parameter of stage i , is obtained from the slope of the straight line of q_t versus $t^{1/2}$. If intraparticle diffusion occurs, then q_t versus $t^{1/2}$ will be linear and if the plot passes through the origin, then the rate limiting process is only due to the intraparticle diffusion. Otherwise, some other mechanism along with intraparticle diffusion is also involved [39]. The plots of intraparticle diffusion model shown in Fig. 8 were not linear over the whole time range, implying that more than one process affected the adsorption. Such finding is similar to that made in previous works on adsorption [40].

3.7. Characterization of GW

Fig. 9a and b shows SEM images for grass adsorbent before adsorption and after 180 min adsorption process, respectively. From Fig. 9a, it is clear that, GW has a rough surface with a heterogeneous pores and cavities. This indicates that there is a good possibility for MB dye to be trapped and adsorbed into the surface.

The FTIR spectra obtained revealed that there were various functional groups detected on the surface of GW. The broad peaks detected at 3434 and 3435 cm⁻¹ (Figure not shown), respectively found in the spectrum of the GW before and after MB adsorption, could be assigned to O–H stretching vibration of hydroxyl functional groups [41,42]. Other functional groups found on both the GW before and after MB adsorption were C–H stretching vibration and NH₂ deformation, respectively recorded at 2852–2923 and 1602–1640 cm⁻¹. However, the intensities of the peaks became weaker after MB adsorption. Other peaks detected on the GW before MB adsorption were located at 1464 and 1164 cm⁻¹, respectively assigned to CH₂ deformation and C–N stretching vibration. Nevertheless, these two functional groups disappeared after MB adsorption.

**Fig. 8.** Intraparticle diffusion plot for adsorption of MB on GW for different initial MB concentrations.

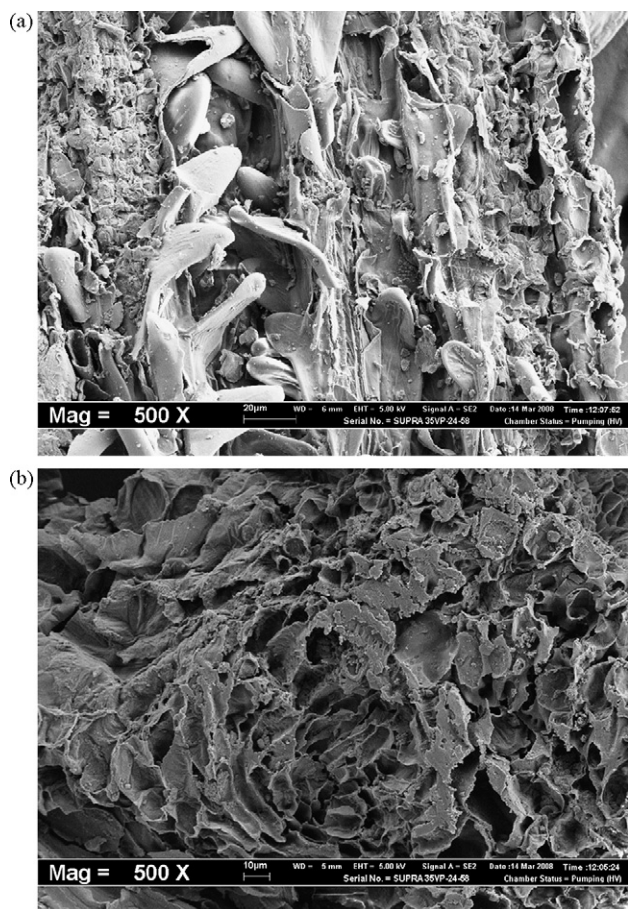


Fig. 9. SEM images for grass adsorbent (a) before adsorption and (b) after 180 min adsorption process (500X).

4. Conclusions

Grass waste sorbent was an effective adsorbent for MB. The equilibrium data were analyzed using the Langmuir and Freundlich isotherms. The data were better described by the Langmuir model. The maximum adsorption capacity obtained was 457.64 mg/g at 30 °C. Kinetic data were adequately fitted by the pseudo-second-order kinetic model. The results of the intraparticle diffusion model suggested that intraparticle diffusion was not the only rate-controlling step.

Acknowledgment

The author thanks his research assistants for their helpful cooperation in the experimental tests.

References

- [1] N.U. Asamudo, A.S. Daba, O.U. Ezeronye, Bioremediation of textile effluent using *Phanerochaete chrysosporium*, Afr. J. Biotechnol. 4 (2005) 1548–1553.
- [2] T. Robinson, G. McMullan, R. Marchant, P. Nigam, Remediation of dyes in textile effluent: a critical review on current treatment technologies with a proposed alternative, Bioresour. Technol. 77 (2001) 247–255.
- [3] B.R. Babu, A.K. Parande, S. Raghu, T.P. Kumar, Cotton textile processing: waste generation and effluent treatment, J. Cotton Sci. 11 (2007) 141–153.
- [4] H. Demir, A. Top, D. Balköse, S. Ülkü, Dye adsorption behavior of *Luffa cylindrica* fibers, J. Hazard. Mater. 153 (2008) 389–394.
- [5] S. Cengiz, L. Cavas, Removal of methylene blue by invasive marine seaweed: *Caulerpa racemosa* var. *cylindracea*, Bioresour. Technol. 99 (2008) 2357–2363.
- [6] S. Şener, Use of solid wastes of the soda ash plant as an adsorbent for the removal of anionic dyes: equilibrium and kinetic studies, Chem. Eng. J. 138 (2008) 207–214.
- [7] Z. Bekçi, C. Özveri, Y. Seki, K. Yurdakoç, Sorption of malachite green on chitosan bead, J. Hazard. Mater. 154 (2008) 254–261.
- [8] P. Pengthamkeerati, T. Satapanajaru, O. Singchan, Sorption of reactive dye from aqueous solution on biomass fly ash, J. Hazard. Mater. 153 (2008) 1149–1156.
- [9] N.A. Oladoja, C.O. Aboluwoye, Y.B. Oladimeji, A.O. Ashogbon, I.O. Otemuyiwa, Studies on castor seed shell as a sorbent in basic dye contaminated wastewater remediation, Desalination 227 (2008) 190–203.
- [10] G. Crini, F. Gimbert, C. Robert, B. Martel, O. Adam, N.M. Crini, F. De Giorgi, P.M. Badot, The removal of Basic Blue 3 from aqueous solutions by chitosan-based adsorbent: batch studies, J. Hazard. Mater. 153 (2008) 96–106.
- [11] B. Bestani, N. Benderdouche, B. Benstaali, M. Belhakem, A. Addou, Methylene blue and iodine adsorption onto an activated desert plant, Bioresour. Technol. 99 (2008) 8441–8444.
- [12] V. Ponnusami, S. Vikram, S.N. Srivastava, Guava (*Psidium guajava*) leaf powder: novel adsorbent for removal of methylene blue from aqueous solutions, J. Hazard. Mater. 152 (2008) 276–286.
- [13] F.A. Pavan, E.C. Lima, S.L.P. Dias, A.C. Mazzocato, Methylene blue biosorption from aqueous solutions by yellow passion fruit waste, J. Hazard. Mater. 150 (2008) 703–712.
- [14] B.H. Hameed, M.I. El-Khaiary, Batch removal of malachite green from aqueous solutions by adsorption on oil palm trunk fibre: equilibrium isotherms and kinetic studies, J. Hazard. Mater. 154 (2008) 237–244.
- [15] B.H. Hameed, Equilibrium and kinetic studies of methyl violet sorption by agricultural waste, J. Hazard. Mater. 154 (2008) 204–212.
- [16] B.H. Hameed, M.I. El-Khaiary, Sorption kinetics and isotherm studies of a cationic dye using agricultural waste: broad bean peels, J. Hazard. Mater. 154 (2008) 639–648.
- [17] M. Arami, N.Y. Limaee, N.M. Mahmoodi, N.S. Tabrizi, Equilibrium and kinetics studies for the adsorption of direct and acid dyes from aqueous solution by soy meal hull, J. Hazard. Mater. B135 (2006) 171–179.
- [18] G. Crini, Non-conventional low-cost adsorbents for dye removal: a review, Bioresour. Technol. 97 (2006) 1061–1085.
- [19] H.W. Yu, Z. Samani, A. Hanson, G. Smith, Energy recovery from grass using two-phase anaerobic digestion, Waste Manag. 22 (2002) 1–5.
- [20] B.H. Hameed, M.I. El-Khaiary, Kinetics and equilibrium studies of malachite green adsorption on rice straw-derived char, J. Hazard. Mater. 153 (2008) 701–708.
- [21] Y. Bulut, H. Aydın, A kinetics and thermodynamics study of methylene blue adsorption on wheat shells, Desalination 194 (2006) 259–267.
- [22] D. Kavitha, C. Namasivayam, Experimental and kinetic studies on methylene blue adsorption by coir pith carbon, Bioresour. Technol. 98 (2007) 14–21.
- [23] C.H. Weng, Y.F. Pan, Adsorption of a cationic dye (methylene blue) onto spent clay, J. Hazard. Mater. 144 (1–2) (2007) 355–362.
- [24] E.N. El Qada, S.J. Allen, G.M. Walker, Adsorption of basic dyes from aqueous solution onto activated carbons, Chem. Eng. J. 135 (2008) 174–184.
- [25] V.V. Basava Rao, S. Ram Mohan Rao, Adsorption studies on treatment of textile dyeing industrial effluent by flyash, Chem. Eng. J. 116 (2006) 77–84.
- [26] S. Wang, Z.H. Zhu, Effects of acidic treatment of activated carbons on dye adsorption, Dyes Pigments 75 (2007) 306–314.
- [27] S. Senthilkumar, P.R. Varadarajan, K. Porkodi, C.V. Subburaam, Adsorption of methylene blue onto jute fiber carbon: kinetics and equilibrium studies, J. Colloid Interface Sci. 284 (2005) 78–82.
- [28] D.S. Faust, M.O. Aly, Chemistry of Wastewater Treatment, Butterworths, Boston, 1983.
- [29] I. Langmuir, The constitution and fundamental properties of solids and liquids, J. Am. Chem. Soc. 38 (11) (1916) 2221–2295.
- [30] H.M.F. Freundlich, Over the adsorption in solution, J. Phys. Chem. 57 (1906) 385–470.
- [31] I.A.W. Tan, A.L. Ahmad, B.H. Hameed, Adsorption of basic dye on high-surface-area activated carbon prepared from coconut husk: equilibrium, kinetic and thermodynamic studies, J. Hazard. Mater. (2008) 337–346.
- [32] B.H. Hameed, A.L. Ahmad, K.N.A. Latiff, Adsorption of basic dye (methylene blue) onto activated carbon prepared from rattan sawdust, Dyes Pigments 75 (2007) 143–149.
- [33] K.R. Hall, L.C. Eagleton, A. Acrivos, T. Vermeulen, Pore- and solid-diffusion kinetics in fixed-bed adsorption under constant-pattern conditions, I&EC Fundam. 5 (1966) 212–223.
- [34] R.E. Treybal, Mass Transfer Operations, 2nd ed., McGraw Hill, New York, 1968.
- [35] Y.S. Ho, G. McKay, Sorption of dye from aqueous solution by peat, Chem. Eng. J. 70 (1998) 115–124.
- [36] S. Lagergren, About the theory of so-called adsorption of soluble substances, K. Sven. Vetenskapsakad. Handl. 24 (4) (1898) 1–39.
- [37] Y.S. Ho, G. McKay, Sorption of dye from aqueous solution by peat, Chem. Eng. J. 70 (1978) 115–124.
- [38] W.J. Weber, J.C. Morris, Kinetics of adsorption on carbon from solution, J. Sanitary Eng. Div. Proceed. Am. Soc. Civil Eng. 89 (1963) 31–59.
- [39] W.H. Cheung, Y.S. Szeto, G. McKay, Intraparticle diffusion processes during acid dye adsorption onto chitosan, Bioresour. Technol. 98 (2007) 2897–2904.
- [40] C.H. Wu, Adsorption of reactive dye onto carbon nanotubes: equilibrium, kinetics and thermodynamics, J. Hazard. Mater. 144 (2007) 93–100.
- [41] M.M. Dávila-Jiménez, M.P. Elizalde-González, A.A. Peláez-Cid, Adsorption interaction between natural adsorbents and textile dyes in aqueous solution, Coll. Surf. A: Physicochem. Eng. Aspects 254 (2005) 107–114.
- [42] K. Mohanty, M. Jha, B.C. Meikap, M.N. Biswas, Biosorption of Cr(VI) from aqueous solutions by *Eichhornia crassipes*, Chem. Eng. J. 117 (2006) 71–77.